Journal of Physics: Conference Series **1342** (2020) 012002 doi:10.1088/1742-6596/1342/1/012002

First results from the CUORE experiment

C. Alduino[1], K. Alfonso[2], F. T. Avignone III[1], O. Azzolini[3], G. Bari[4], F. Bellini[5,6], G. Benato[7], A. Bersani[8], M. Biassoni[9], A. Branca[10,11], C. Brofferio[12,9], C. Bucci[13], A. Camacho[3], A. Caminata[8], L. Canonica[14,13], X. G. Cao[15], S. Capelli[12,9], L. Cappelli[7,16,13], L. Cardani[6], P. Carniti[12,9], N. Casali[6], L. Cassina[12,9], D. Chiesa[12,9], N. Chott[1], M. Clemenza[12,9], S. Copello[17,8], C. Cosmelli[5,6], O. Cremonesi[9,b], R. J. Creswick[1], J. S. Cushman[18], A. D'Addabbo[13], D. D'Aguanno[13,19], I. Dafinei[6], C. J. Davis[18], S. Dell'Oro[20], M. M. Deninno[4], S. Di Domizio[17,8], M. L. Di Vacri[13,21], V. Dompè[13,22], A. Drobizhev[7,16], D. Q. Fang[15], M. Faverzani[12,9], E. Ferri[9], F. Ferroni[5,6], E. Fiorini[9,12], M. A. Franceschi[23], S. J. Freedman[16,7,a], B. K. Fujikawa[16], A. Giachero[12,9], L. Gironi[12,9], A. Giuliani[24], L. Gladstone[14], P. Gorla[13], C. Gotti[12,9], T. D. Gutierrez[25], K. Han[26], K. M. Heeger[18], R. Hennings-Yeomans[7,16], H. Z. Huang[2], G. Keppel[3], Yu. G. Kolomensky[7,16], A. Leder[14], C. Ligi[23], K. E. Lim[18], Y. G. Ma[15], L. Marini[17,8], M. Martinez[5,6,27], R. H. Maruyama[18], Y. Mei[16], N. Moggi[28,4], S. Morganti[6], S. S. Nagorny[13,22], T. Napolitano[23], M. Nastasi[12,9], C. Nones[29], E. B. Norman[30,31], V. Novati[24], A. Nucciotti[12,9], I. Nutini[13,22], T. O'Donnell[20], J. L. Ouellet[14], C. E. Pagliarone[13,19], M. Pallavicini[17,8], V. Palmieri[3], L. Pattavina[13], M. Pavan[12,9], G. Pessina[9], C. Pira[3], S. Pirro[13], S. Pozzi[12,9], E. Previtali[9], F. Reindl[6], C. Rosenfeld[1], C. Rusconi[1,13], M. Sakai[2], S. Sangiorgio[30], D. Santone[13,21], B. Schmidt[16], J. Schmidt[2], N. D. Scielzo[30], V. Singh[7], M. Sisti[12,9], L. Taffarello[10], F. Terranova[12,9], C. Tomei[6], M. Vignati[6], S. L. Wagaarachchi[7,16], B. S. Wang[30,31], H. W. Wang[15], B. Welliver[16], J. Wilson[1], K. Wilson[1], L. A. Winslow[14], T. Wise[18,32], L. Zanotti[12,9], G. Q. Zhang[15], S. Zimmermann[33], and S. Zucchelli[28,4]

[1] Department of Physics and Astronomy, University of South Carolina, Columbia, SC 29208, USA
[2] Department of Physics and Astronomy, University of California, Los Angeles, CA 90095, USA
[3] INFN – Laboratori Nazionali di Legnaro, Legnaro (Padova) I-35020, Italy
[4] INFN – Sezione di Bologna, Bologna I-40127, Italy
[5] Dipartimento di Fisica, Sapienza Università di Roma, Roma I-00185, Italy
[6] INFN – Sezione di Roma, Roma I-00185, Italy
[7] Department of Physics, University of California, Berkeley, CA 94720, USA
[8] INFN – Sezione di Genova, Genova I-16146, Italy
[9] INFN – Sezione di Milano Bicocca, Milano I-20126, Italy
[10] INFN – Sezione di Padova, Padova I-35131, Italy
[11] Dipartimento di Fisica e Astronomia, Università di Padova, I-35131 Padova, Italy
[12] Dipartimento di Fisica, Università di Milano-Bicocca, Milano I-20126, Italy
[13] INFN – Laboratori Nazionali del Gran Sasso, Assergi (L'Aquila) I-67100, Italy
[14] Massachusetts Institute of Technology, Cambridge, MA 02139, USA
[15] Shanghai Institute of Applied Physics, Chinese Academy of Sciences, Shanghai 201800, China
[16] Nuclear Science Division, Lawrence Berkeley National Laboratory, Berkeley, CA 94720, USA
[17] Dipartimento di Fisica, Università di Genova, Genova I-16146, Italy
[18] Wright Laboratory, Department of Physics, Yale University, New Haven, CT 06520, USA
[19] Dipartimento di Ingegneria Civile e Meccanica, Università degli Studi di Cassino e del Lazio Meridionale, Cassino I-03043, Italy

[20] Center for Neutrino Physics, Virginia Polytechnic Institute and State University, Blacksburg, Virginia 24061, USA
[21] Dipartimento di Scienze Fisiche e Chimiche, Università dell'Aquila, L'Aquila I-67100, Italy
[22] INFN – Gran Sasso Science Institute, L'Aquila I-67100, Italy
[23] INFN – Laboratori Nazionali di Frascati, Frascati (Roma) I-00044, Italy
[24] CSNSM, Univ. Paris-Sud, CNRS/IN2P3, Universit Paris-Saclay, 91405 Orsay, France
[25] Physics Department, California Polytechnic State University, San Luis Obispo, CA 93407, USA
[26] INPAC and School of Physics and Astronomy, Shanghai Jiao Tong University; Shanghai Laboratory for Particle Physics and Cosmology, Shanghai 200240, China
[27] Laboratorio de Fisica Nuclear y Astroparticulas, Universidad de Zaragoza, Zaragoza 50009, Spain
[28] Dipartimento di Fisica e Astronomia, Alma Mater Studiorum – Università di Bologna, Bologna I-40127, Italy
[29] Service de Physique des Particules, CEA / Saclay, 91191 Gif-sur-Yvette, France
[30] Lawrence Livermore National Laboratory, Livermore, CA 94550, USA
[31] Department of Nuclear Engineering, University of California, Berkeley, CA 94720, USA
[32] Department of Physics, University of Wisconsin, Madison, WI 53706, USA
[33] Engineering Division, Lawrence Berkeley National Laboratory, Berkeley, CA 94720, USA

[a] Deceased
[b] email: oliviero.cremonesi@mib.infn.it

Abstract. CUORE (Cryogenic Underground Observatory for Rare Events) is a ton-scale experiment aiming to the search of neutrino-less double beta decay in ^{130}Te with a projected sensitivity on the Majorana effective mass close to the inverted hierarchy region. The CUORE detector consists of a segmented array of 988 TeO_2 bolometers, organized in 19 towers and operated at a temperature of about 10 mK thanks to a custom cryogenic system which, besides the uncommon scale, observes several constraints from the radio-purity of the materials to the mechanical decoupling of the cooling systems. The successful commissioning of the CUORE cryogenic system has been completed early in 2016 and represents an outstanding achievement by itself. The installation of the detector proceeded along 2016 followed by the cooldown to base temperature at the beginning of 2017. The CUORE detector is now operational and has been taking science data since Spring 2017. With the first ∼3 weeks of collected data, we present here the most stringent constraint on the ^{130}Te half-live for the neutrino-less double beta decay.

Neutrinoless double-beta decay ($\beta\beta(0\nu)$), is a very rare process in which a nucleus with mass number A and charge Z undergoes the decay $(A, Z) \rightarrow (A, Z + 2) + 2e^-$ in which no neutrino is emitted. Assuming that the process is mediated by the exchange of a light neutrino, $\beta\beta(0\nu)$ provides the most sensitive test of the Majorana nature of neutrinos [1]. While the corresponding two-neutrino double-beta decay ($\beta\beta(2\nu)$) has been observed for several nuclides [2], the observation of $\beta\beta(0\nu)$ would provide direct evidence for lepton number violation implying the existence of new physics beyond the Standard Model. In addition it would constrain the absolute neutrino mass scale [3]. A variety of experiments are therefore searching for $\beta\beta(0\nu)$ in a number of nuclides, reaching half-life sensitivities close to 10^{26} years [3, 4].

The Cryogenic Underground Observatory for Rare Events (CUORE) [5] is an experiment searching for $\beta\beta(0\nu)$ decay in ^{130}Te . It is located at the Laboratori Nazionali del Gran Sasso (LNGS) of INFN, in central Italy. The CUORE detector consists of 988 cubic TeO_2 crystals with natural ^{130}Te isotopic abundance (34.2 %), 5 cm side and a 750 g average mass, operated as bolometers at very low temperature around 10 mK.

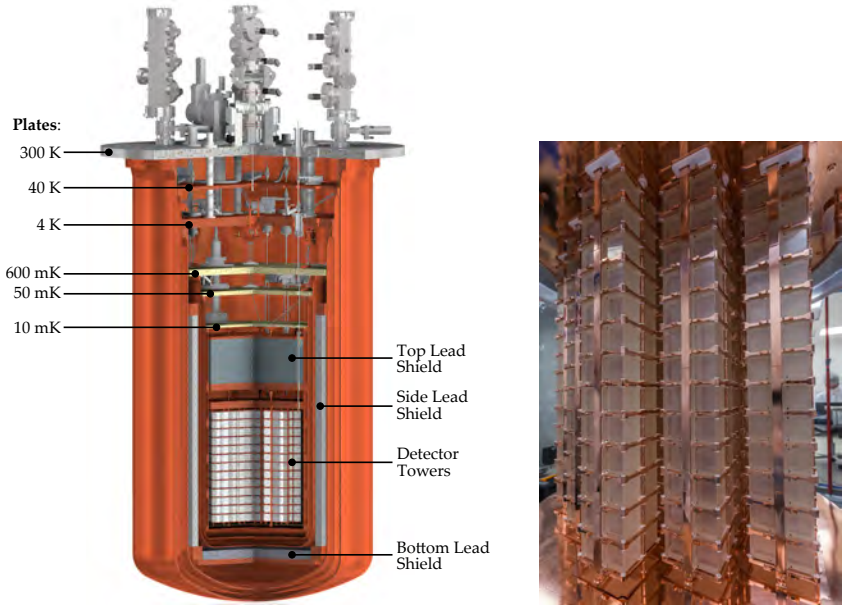

Figure 1. An illustration of the CUORE cryostat (left) and a picture of the CUORE detector (right).

The 988 TeO_2 bolometers are arranged into 19 towers, each consisting of 13 floors of 4 detectors (Fig. 1 right).

The towers are arranged in a close-packed array and thermally connected to the mixing chamber of a ^{3}He/^{4}He dilution refrigerator (Leiden Cryogenics DRS-CF3000 continuous-cycle). The cooling of the system at intermediate temperatures (∼40 K and ∼4 K) is based on five pulse tube cryocoolers (Cryomech PT415-RM) with a Joule-Thomson expansion valve. The dimensions, experimental volume (∼1 m^3), mass (∼17 t), and cooling power (3 μW at 10 mK) make this the largest and most powerful cryogen-free dilution cryostat in operation [6] (Fig. 1 left). To minimize transmission of vibrations from the cryostat to the bolometers, the detector towers are independently supported by a Y-shaped beam that is vibrationally isolated from the cryostat support structure [7]. The cryostat and detector supporting systems, as well as the front-end electronics are located together in a Faraday Room [8] at the second floor of the CUORE underground building.

After the successful installation of the detector in the summer 2016, CUORE started the commissioning phase at the beginning of 2017. The initial two months were dedicated to the system optimization and setting of the optimal working points. In April 2017 the optimization phase was not yet complete but CUORE was eventually ready for a preliminary science run.

The data presented here are from a three week-long dataset collected in May 2017 and corresponding to an exposure of 38.1 kg·yr of TeO_2 or 10.6 kg·yr of $^{130}TeO_2$. Main goal of this preliminary physics run was to provide preliminary information on the parameters that most strongly affect the $\beta\beta(0\nu)$ sensitivity: the energy resolution and the Background Index (BI) in the $\beta\beta(0\nu)$ Region Of Interest (ROI). Physics data were preceded and followed by calibration periods during which 12 Kevlar strings populated with low-intensity ^{232}Th sources were temporarily deployed (from room temperature across the cryogenic volume) inside the detector region in order to guarantee an approximately uniform γ-ray illumination of the detectors [9]. Main goal of the closing calibration is to verify the stability of the detector response over the dataset.

A total of 984 of 988 detectors are functioning. Each CUORE detector is equipped with

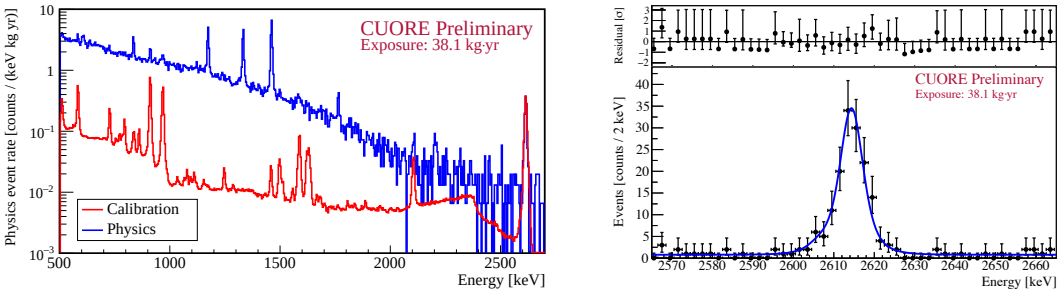

Figure 2. Left: Reconstructed energy spectra of physics (blue) and calibration (red) data. The calibration spectrum is normalized to the physics data at the 2615-keV line. Right: Detail of the 2615-keV line in the physics data. The fitted energy resolution is 7.9 ± 0.6 keV FWHM.

a neutron-transmutation-doped (NTD) thermistor [10], and a silicon heater [11, 12]. During data collection, the voltage across each thermistor is amplified and filtered [13] and continuously digitized with a sampling rate of 1 kHz. A software derivative trigger with channel-dependent thresholds ranging from 20 to a few hundred keV is applied to identify thermal pulses. The efficiency of the trigger is evaluated as the fraction of tagged heater pulses that produce an event trigger.

The rise and fall times of thermal pulses are on the order of 100 ms and 400 ms, respectively. A 5-s window, consisting of 1 s before and 4 s after each trigger, is separately analyzed for each triggered pulse. The pre-trigger voltage provides a proxy for the bolometer temperature before the event, while the pulse amplitude returns the energy of the event.

To improve the signal-to-noise ratio, we apply an optimal filter to each pulse [14].

A dedicated electrical circuit with a thermal feedbacked is used to inject power on the dilution unit plate to maintain a stable predetermined operating temperature. In order to correct for residual temperature instabilities)which could otherwise spoil the energy resolution of our detectors) a stable voltage pulse [15] is injected into the silicon heater on each bolometer, every few minutes, to generate tagged reference events with fixed thermal energy[11]. This heater-based thermal gain stabilization (heater-TGS) cannot be applied to bolometers without functioning heaters. In these cases we apply a second method based on pulses induced by γ rays from the 2615-keV ^{208}Tl calibration line (calibration-TGS). Calibration-TGS is also used when a statistically significant improvement in sensitivity is obtained with respect to heater-TGS. Both methods were developed and used in CUORE-0 [16].

Six γ lines from the ^{232}Th calibration sources ranging from 239 keV to 2615 keV are used to calibrate the detectors. A second-order polynomial with zero constant term provides a good description of the calibration functions of each bolometer throughout the calibrated energy range.

After applying the calibration , the physics data are blinded for the subsequent analysis. This is obtained by introducing an artificial peak at $Q_{\beta\beta}$ [16]. The calibration and unblinded physics spectra are shown in fig. 2.

To select $\beta\beta(0\nu)$ decay candidates in the physics data, we apply a series of selection criteria ("base selection"): after discarding noisy periods caused by laboratory conditions, we require a single pulse-like feature in the event window and a stable thermistor voltage prior to the event trigger. In addition, only waveforms consistent with a proper template are selected (pulse shape analysis). These are characterized with six pulse-shape parameters and represent each event with a point in a 6-dimensional space. The Mahalanobis distance D_M [17] from the mean position of the signal sample, is then calculated for each event. The upper limit on D_M that

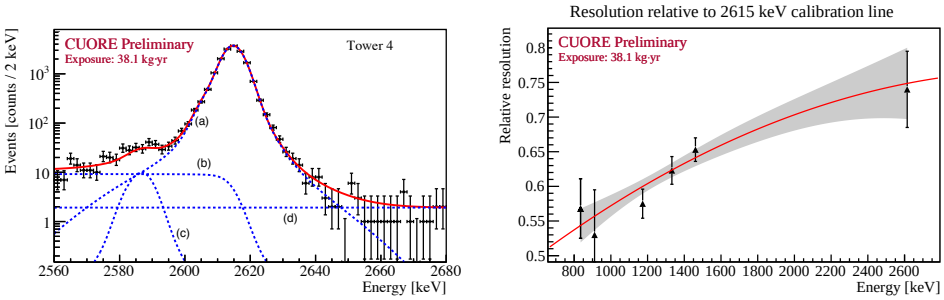

Figure 3. Left: Sum over the detectors of a tower (n. 4) of the UEML fits to the 2615 keV line in calibration data (solid line). The different components of the line shape model are also shown by the dashed lines: (a) the multi-Gaussian photopeak describing the detector response function, (b) a multiscatter Compton contribution, (c) multiple peaks due to 27–31 keV Te X-ray escapes, (d) a linear continuum background due to coincident event. Right: scaling curve for the energy resolution in the physics data with respect to the 2615 keV calibration line.

maximizes the discovery sensitivity [18] is eventually calculated using ^{40}K events near 1461 keV. No data from the $\beta\beta(0\nu)$ ROI are used throughout the optimization process. The efficiency of the pulse shape selection is eventually evaluated using events belonging to the ^{208}Tl 2615-keV line.

Events occurring within 10 ms of another event in a different bolometer in the array are discarded in order to reduce backgrounds from events depositing energy in multiple crystals (e.g., α particles on crystal surfaces or multiple Compton scatters of γ rays). This is referred as "multiplicity 1" (M1) or anti-coincidence selection. The corresponding efficiency has two components: a probability for a $\beta\beta(0\nu)$ decay to be fully contained in a single crystal ("containment efficiency") and a probability for it to not be accidentally coincident with another event ("pulse selection efficiency"). The former (88.35 ± 0.09 %) is estimated from simulation [19, 20] while the latter ($62.6 \pm 3.4\%$) is evaluated on the 1461-keV γ ray from ^{40}K electron capture and combines the contributions from the base ($98.47 \pm 0.01\%$), pulse shape ($64 \pm 3\%$) and anti-coincidence ($99.3 \pm 0.3\%$) efficiencies. The combined cumulative (single channel) efficiency is then averaged over all channels with functioning heaters and applied to all the channels.

The energy threshold for coincident events has been set to 150 keV to avoid uncontrolled effects in the ROI due to the spread of the trigger thresholds. We expect to lower this in the future as we improve the operating conditions of the experiment.

A total of 889 detectors (∼90 %) were used for this initial analysis.

In order to establish the detector response in the ROI we use the high-statistics ^{208}Tl 2615-keV γ line from calibration data. The CUORE detectors exhibit a slightly non-Gaussian line shape, already observed in CUORE-0 [16] and Cuoricino [21, 22], whose origin is still under investigation. We model it therefore empirically with a primary Gaussian component centered at 2615 keV and two additional Gaussian components, on the right and left side of the main peak. The choice of this line shape (the one that provides the best desciption of the data) is treated as a systematic uncertainty. All three Gaussian components are parametrized with the same width. We estimate the line shape parameters in each tower with a simultaneous, unbinned extended maximum likelihood (UEML) fit performed on the detectors of that tower (Fig. 3 left).

We observe a systematic differences in the detector energy resolutions between the calibration and physics runs (likely due to the higher event rate during calibration). In particular the armonic mean of the detector FWHM resolutions on the 2615 keV line in calibration runs is

10.6 keV while the fitted FWHM in the physics runs is 7.9 ± 0.6 keV. To account for this, we apply a global scaling factor to the width parameter of each detector in the physics runs. We model its energy dependence as a quadratic function, whose parameters are determined from a simultaneous UEML fit to the most prominent lines in the physics spectrum (Fig. 3 right). The value at $Q_{\beta\beta}$ is 0.74 ± 0.06.

The model and fitting strategy for the analysis of the ^{130}Te $\beta\beta(0\nu)$ ROI (2465–2575 keV) are fixed before the unblinding of the physics data. In particular, the model is the same used for CUORE-0 [16] and is composed of a posited $\beta\beta(0\nu)$ decay peak, a peak for ^{60}Co coincident γ rays (1173 and 1332 keV), and a flat background. Each peak in the ROI is modeled using the calibration line shape discussed above, with the line width scaled by the resolution scaling parameter extrapolated to the peak energy. All detectors are constrained to have the same $\beta\beta(0\nu)$ decay rate $\Gamma_{0\nu}$, which we allow to vary freely in the fit; the position of the $\beta\beta(0\nu)$ decay peak is fixed to the reconstructed energy of $Q_{\beta\beta}$ for each bolometer-dataset. The ^{60}Co peak mean and rate, as well as the flat background rate are free parameters in the fit. Fig. 4 shows the spectrum of candidate events in the $\beta\beta(0\nu)$ ROI after unblinding, together with the result of the UEML fit. The best-fit values in the ROI are $0.98^{+0.17}_{-0.15}\times10^{-2}$ counts/(keV·kg·y) for the BI and $(-0.03^{+0.07}_{-0.04}\ \text{(stat.)} \pm 0.01\ \text{(syst.)}) \times 10^{-24}$ yr^{-1} for the $\Gamma_{0\nu}$.

We estimate the systematic uncertainties following the same procedure used for CUORE-0 [16]. The most relevant sources of scaling systematic errors come from the line shape (1.7 %), the energy resolution (1.2 %) and the selection efficiency (5.4 %). The line shape and the energy scales give also an additive contribution of 8×10^{-27} and 7×10^{-27} yr^{-1}.

Our data do not show any evidence for $\beta\beta(0\nu)$ decay of ^{130}Te and we can only set a 90% C.L. upper limit equal to $\Gamma_{0\nu} < 0.15 \times 10^{-24}$ yr^{-1} (stat. only) on $\Gamma_{0\nu}$, by integrating the profile likelihood in the physical region ($\Gamma_{0\nu} \geq 0$). This corresponds to a half-life lower limit of $T^{0\nu}_{1/2} > 4.5 \times 10^{24}$ yr, including systematics. this has to be compared with a median expected sensitivity of 3.6×10^{24} yr [23]. The analysis described above has been carried out using the RooFit toolkit [24] with the Minuit minimization routines [25]. An independent frequentist analysis [26] yields $T^{0\nu}_{1/2} > 6.1 \times 10^{24}$ yr at 90% C.L.

By combining the CUORE profile NLL curve with those from 9.8 kg·yr of ^{130}Te exposure from CUORE-0 [27] and 19.8 kg·yr from Cuoricino [28] (see fig. 4 right) we get a combined 90% C.L. limit $T^{0\nu}_{1/2} > 6.6 \times 10^{24}$ yr. The frequentist technique yields $T^{0\nu}_{1/2} > 8.1 \times 10^{24}$ yr.

The combined half-life limit, $T^{0\nu}_{1/2} > 6.6 \times 10^{24}$ yr, can be then interpreted as a limit on the effective Majorana neutrino mass ($m_{\beta\beta}$) in the framework of models of $\beta\beta(0\nu)$ decay mediated by light Majorana neutrino exchange. When using the phase-space factors from [29] and nuclear matrix elements from a broad range of recent calculation models [30, 31, 32, 33, 34] with the nucleon axial coupling constant $g_A \simeq 1.27$ we get $m_{\beta\beta} < (210-590)$ meV at 90% C.L., depending on the nuclear matrix element estimates employed.

In summary, we find no evidence for $\beta\beta(0\nu)$ decay of ^{130}Te and place the most stringent limit to date on the half-life for this decay. We anticipate additional optimization campaigns during 2017 to improve the detector performance by optimizing our experimental operating conditions and analysis tools.

Note added in proof: a new science run was carried out during August 2017. The corresponding dataset as well as the one described in this paper were completely re-processed with a slightly improved analysis procedure. The corresponding results have been recently submitted for publication to PRL [35].

The CUORE Collaboration thanks the directors and staff of the Laboratori Nazionali del Gran Sasso and our technical staff for their valuable contribution to building and operating

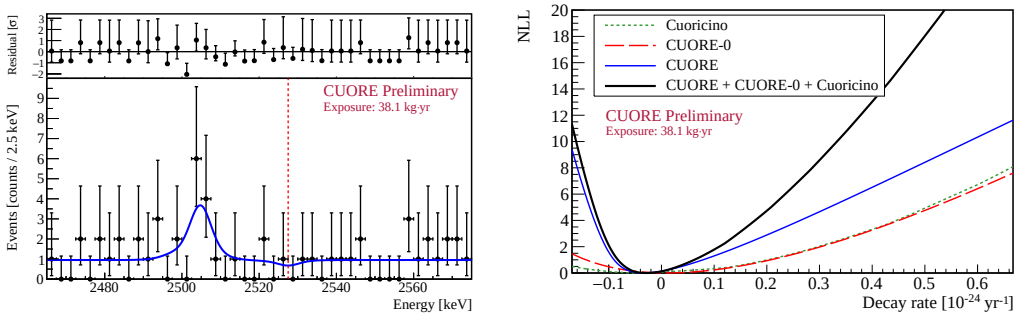

Figure 4. Left: Best-fit model from the UEML fit (solid blue line) overlaid on the spectrum of $\beta\beta(0\nu)$ decay candidates observed in CUORE. The peak near 2506 keV is attributed to ^{60}Co [16]. Right: Profile negative-log-likelihood curves for CUORE, CUORE-0, Cuoricino, and their combination..

the detector. We thank Danielle Speller for contributions to detector calibration, data analysis, and discussion of the manuscript. We thank Giorgio Frossati for his crucial support in the commissioning of the dilution unit. This work was supported by the Istituto Nazionale di Fisica Nucleare (INFN); the National Science Foundation under Grant Nos. NSF-PHY-0605119, NSF-PHY-0500337, NSF-PHY-0855314, NSF-PHY-0902171, NSF-PHY-0969852, NSF-PHY-1307204, and NSF-PHY-1404205; the Alfred P. Sloan Foundation; and Yale University. This material is also based upon work supported by the US Department of Energy (DOE) Office of Science under Contract Nos. DE-AC02-05CH11231 and DE-AC52-07NA27344; and by the DOE Office of Science, Office of Nuclear Physics under Contract Nos. DE-FG02-08ER41551, DE-FG03-00ER41138, DE-SC0011091, and DE-SC0012654. This research used resources of the National Energy Research Scientific Computing Center (NERSC).

References

[1] E. Majorana. *Nuovo Cimento*, 14:171, 1937.

[2] C. Patrignani et al. (Particle Data Group). *Chin. Phys. C*, 40:100001, 2016.

[3] S. Dell'Oro, S. Marcocci, M. Viel, and F. Vissani. *Adv. High Energy Phys.*, 2016:2162659, 2016.

[4] O. Cremonesi and M. Pavan. *Adv. High Energy Phys.*, 2014:951432, 2013.

[5] R. Ardito et al. Cuore: A cryogenic underground observatory for rare events, 2005. arxiv:hep-ex/0501010.

[6] F. Alessandria et al. The cuore cryostat: A 10 mk infrastructure for large bolometric arrays. In preparation.

[7] A. Bersani et al. The detector suspension system of the cuore experiment. In preparation.

[8] C. Bucci et al. The faraday room of the cuore experiment. arxiv:1710.05614.

[9] J. S. Cushman et al. *Nucl. Instrum. Meth. A*, 844:32, 2017.

[10] D. McCammon. *Top. Appl. Phys.*, 99:35, 2005.

[11] A. Alessandrello et al. *Nucl. Instrum. Meth. A*, 412:454, 1998.

[12] E. Andreotti et al. *Nucl. Instrum. Meth. A*, 664:161, 2012.

[13] C. Arnaboldi, P. Carniti, L. Cassina, C. Gotti, X. Liu, and G. Pessina. The front end electronics system for the cuore experiment. In preparation.

[14] E. Gatti and P. F. Manfredi. *Nuovo Cimento*, 9.

[15] P. Carniti, L. Cassina, A. Giachero, C. Gotti, and G. Pessina. A high precision pulse generation and stabilization system for bolometric experiments, 2017. arxiv:1710.05565.

[16] C. Alduino et al. (CUORE Collaboration). *Phys. Rev. C*, 93:045503, 2016.

[17] P. C. Mahalanobis. *Proc. Natl. Inst. Sci. India*, page 49, 1936.

[18] G. Cowan, K. Cranmer, E. Gross, and O. Vitells. *Eur. Phys. J. C*, 71:1554, 2011.

[19] S. Agostinelli et al. *Nucl. Instr. Meth. A*, page 250, 2003.

[20] C. Alduino et al. (CUORE Collaboration). *Eur. Phys. J. C*, 77:543, 2017.

[21] A. D. Bryant. *A Search for Neutrinoless Double Beta Decay of* $^{1}30\,Te$. PhD thesis, University of California, Berkeley, 2010.

[22] M. Carrettoni. *Data analysis for Neutrinoless Double Beta Decay.* PhD thesis, Università degli Studi di Milano-Bicocca, 2011.

[23] C. Alduino et al. (CUORE Collaboration). *Eur. Phys. J. C*, 77:532, 2017.

[24] W. Verkerke and D. P. Kirkby. The roofit toolkit for data modeling. physics/0306116, 2003.

[25] F. James and M. Roos. *Comput. Phys. Commun.*, 10:343, 1975.

[26] W. A. Rolke, A. M. Lopez, and J. Conrad. *Nucl. Instrum. Meth. A*, 551:493, 2005.

[27] K. Alfonso et al. (CUORE Collaboration). *Phys. Rev. Lett.*, 115:102502, 2015.

[28] E. Andreotti et al. *Astropart. Phys.*, 34:822, 2011.

[29] J. Kotila and F. Iachello. *Phys. Rev. C*, 85:034316, 2012.

[30] J. Barea, J. Kotila, and F. Iachello. *Phys. Rev. C*, 91:034304, 2015.

[31] F. Simkovic, V. Rodin, A. Faessler, and P. Vogel. *Phys. Rev. C*, 87:045501, 2013.

[32] J. Hyvarinen and J. Suhonen. *Phys. Rev. C*, 91:024613, 2015.

[33] J. Menendez, A. Poves, E. Caurier, , and F. Nowacki. *Nucl. Phys. A*, 818:139, 2009.

[34] T. R. Rodriguez and G. Martinez-Pinedo. *Phys. Rev. Lett.*, 105:252503, 2010.

[35] C.Alduino et al. (CUORE Collaboration), 2017. arxiv:1710.07988. Submitted for publication to Phys. Rev. Lett.